

Visible and near-infrared absorption spectroscopy by an integrating sphere and optical fibers for quantifying and discriminating the adulteration of extra virgin olive oil from Tuscany

Anna Grazia Mignani · Leonardo Ciaccheri · Heidi Ottevaere · Hugo Thienpont · Lanfranco Conte · Milena Marega · Angelo Cichelli · Cristina Attilio · Antonio Cimato

Received: 2 August 2010 / Revised: 29 October 2010 / Accepted: 2 November 2010 / Published online: 24 November 2010
© Springer-Verlag 2010

Abstract Because of its high price, extra virgin olive oil is frequently targeted for adulteration with lower quality oils. This paper presents an innovative optical technique capable of quantifying and discriminating the adulteration of extra virgin olive oil caused by lower-grade olive oils. An original set-up for diffuse-light absorption spectroscopy in the wide 400–1,700 nm spectral range was experimented. It made use of an integrating sphere containing the oil sample and of optical fibers for illumination and detection; it provided intrinsically scattering-free absorption spectroscopy measurements. This set-up was used to collect spectro-

scopic fingerprints of authentic extra virgin olive oils from the Italian Tuscany region, adulterated by different concentrations of olive-pomace oil, refined olive oil, deodorized olive oil, and refined olive-pomace oil. Then, a straightforward multivariate processing of spectroscopic data based on principal component analysis and linear discriminant analysis was applied which was successfully capable of predicting the fraction of adulterant in the mixture, and of discriminating its type. The results achieved by means of optical spectroscopy were compared with the analysis of fatty acids, which was carried out by standard gas chromatography.

A. G. Mignani · L. Ciaccheri (✉)
CNR-IFAC,
Via Madonna del Piano, 10-Building B,
50019 Sesto Fiorentino, FI, Italy
e-mail: l.ciaccheri@ifac.cnr.it

H. Ottevaere · H. Thienpont
Vrije Universiteit Brussel,
B-PHOT, Pleinlaan, 2,
1050 Brussels, Belgium

L. Conte · M. Marega
Università degli Studi di Udine,
Dipartimento di Scienze degli Alimenti,
Via Sondrio, 2A,
33100 Udine, Italy

A. Cichelli
Università degli Studi “G. D’Annunzio”, DASTA,
Viale Pindaro, 42,
65127 Pescara, Italy

C. Attilio · A. Cimato
CNR-IVALSA,
Via Madonna del Piano, 10-Building D,
50019 Sesto Fiorentino, FI, Italy

Keywords Extra virgin olive oil · Absorption spectroscopy · Integrating cavity · Optical fibers · Adulteration · Chemometrics

Protecting the authentic extra virgin olive oil

Extra virgin olive oil (EVOO) is the only vegetable oil that is consumed as it is—freshly extracted from the fruit. Thanks to its balanced taste and flavored aroma, EVOO is capable of enhancing the most popular gastronomic recipes and is thus considered the chef’s gold. EVOO also offers highly beneficial health effects, thanks to both its high content of monounsaturated fatty acids, vitamins, and polyphenols—the antioxidant substances.

EVOO extraction, being carried out by mechanical means only, preserves the contents of antioxidant compounds. Some of these molecules are not contained in other vegetable oils (e.g. polyphenols), or are removed by refining, while those that are contained in every vegetable oil (tocopherols) are partially removed by refining. Seed

oils usually undergo to refining both because of inadequate characteristics to direct human consumption and with the aim to fit standards.

Among all vegetable oils, EVOO contains the highest levels of antioxidants and the highest amount of monounsaturated fatty acids. It is a “healing fat”, since it controls the “bad” LDL cholesterol levels while raising the “good” HDL ones [1, 2]. Studies have shown that people who consumed 25 ml—about two tablespoons—of EVOO daily for 1 week presented less oxidation of LDL cholesterol and higher levels of antioxidant compounds in the blood [3], and, more generally, that EVOO is a panacea of the entire cardiovascular system [4].

Because of the time-consuming agronomical practices used for EVOO production, and the low production efficiency—frequently lower than 20% as oil yield—the price of EVOO is high, especially compared with that of other vegetable oils. Consequently, EVOO is prone to adulteration with cheaper oils in order to increase profits. In addition to an economic burden, EVOO adulteration is detrimental if consumers react by buying other cooking fats or dressings, thinking that EVOO cannot be trusted. The negative implications on consumer confidence are even worse than the economic ones. Lastly, EVOO protection measures also imply the product area conservation, as far as landscape, tourism, and job preservation are concerned.

While the European Commission regulations are indicating the characteristics of olive oil types, and are suggesting the methods of analysis [5], a lot of research is currently carried out, in order to experiment innovative techniques for authenticating extra virgin olive oils and predicting potential frauds.

Numerous methodologies exist for EVOO authentication, both for adulteration detection and quantification. Chromatographic, nuclear magnetic resonance and thermal techniques are frequently used, as well as dielectric spectroscopy or electronic noses [6–15]. They are mostly suitable for laboratory use, since the instrumentation is cumbersome and some treatments of the analyzed sample are required. Optical spectroscopy is also frequently used and sometimes preferred because it allows a rapid and non-destructive analysis and requires minimum or no sample preparation. Infrared, mid-infrared, and fluorescence spectroscopic techniques have been proposed, as well as absorption spectroscopy in the ultraviolet, visible, or near-infrared spectral ranges [16–24]. These optical techniques are usually combined with chemometric methods for spectroscopic data processing, thus providing an excellent EVOO authentication [25–28]. Currently, the intrinsic optical and mechanical characteristics of optical fibers, together with the wide availability of bright LEDs and miniaturized spectrometers, further enhance the potentials of absorption spectroscopy in the visible and near-infrared

spectral ranges, and make possible the implementation of compact instrumentation. However, none of the absorption spectroscopy techniques experimented so far takes into account the intrinsic turbidity of the olive oil, which can considerably impair absorption measurements because of the unavoidable attenuation due to the scattering produced by suspended particles.

Indeed, although the intrinsic turbidity of the oil can be regarded as a peculiar characteristic, it has an unstable and non-reproducible influence on absorption measurements because of its time-dependent nature. In fact, suspended particles created during production of the olive oil usually settle down in a non-reversible way, because they tend to aggregate at the bottom of the container, creating a sort of sludge. Sample filtering is not only a time-consuming procedure, but is also an action that alters the composition of the sample. In fact, turbidity is also due to the presence of water, and water removal causes a serious loss of water-soluble compounds—such as polyphenols—that are responsible for the unusual character and authenticity of olive oil.

This paper shows an absorption spectroscopy experiment, carried out in the wide 400–1,700 nm spectral range by means of optical fiber technology, for predicting the adulteration of authentic EVOO produced in the Italian region of Tuscany caused by lower-grade olive oil. EVOO produced in Tuscany is highly appreciated by consumers thanks to its mild fruity aroma with a touch of artichoke, thistle, and grass. It is expensive, being produced at the early ripening of olives. EVOO is one of the most important and popular agricultural products of the region. Actually, one of the main actions of the Regional Board of Tuscany is the protection of EVOO, which is also carried through the early detection of commercial frauds.

Olive-pomace oil (OPO), refined olive-pomace oil (ROPO), refined olive oil (ROO), and deodorized olive oil (DOO) were considered as adulterants. While the detection of EVOO adulteration caused by ROPO, and ROO has been previously achieved by means of absorption spectroscopy [29], we innovatively tested the adulteration caused by DOO, an emerging adulterant, the detection of which is hard to achieve by means of conventional techniques. For the first time, to the best of our knowledge, the spectral fingerprints of authentic and adulterated EVOOs were obtained by means of diffuse-light absorption spectroscopy, which provided intrinsically scattering-insensitive measurements. Then, a customized multivariate processing of spectroscopic data was applied for a straightforward prediction of adulterant concentration and identification of adulterant type.

In order to evaluate the effectiveness of optical spectroscopy as compared to other standard methods, a gas chromatographic analysis of fatty acid composition was also carried out. The results obtained by means of an optical

analysis were comparable with those provided by the standard technique, thus demonstrating the validity of an optical approach.

Diffuse-light absorption spectroscopy: the principle and set-up

Absorption spectroscopy in the visible and near-infrared spectral regions is one of the most popular measuring methods of conventional analytic chemistry [30, 31]. More recently, absorption spectra measured in wide spectral ranges, like in the visible and near-infrared, have been considered as signatures or fingerprints from which to predict quality indicators of the product by means of multivariate data processing or other chemometric methods [32]. An added value to absorption spectroscopy is the use of optical fiber technology, since it allows real time and in situ measurements.

When carrying out absorption spectroscopy in liquids, the measurements are found to be influenced by dispersed scattering particles that cause turbidity. Scattering dependence is the main drawback of absorption spectroscopy, especially when particles settle down, or change their position in time. For this reason, liquids must be filtered prior to measurements, with a consequent loss of time and increased costs.

Diffuse-light absorption spectroscopy, that is, spectroscopy carried out by means of an integrating cavity, has been proposed in the literature as an effective method for overcoming scattering-dependence problems in process control [33] and biological applications [34], as well as for more general quantitative spectrophotometry [35].

Diffuse-light absorption spectroscopy makes use of an integrating cavity, typically an integrating sphere which contains the sample under test. The source and the detector are butt-coupled to the sphere. Almost all the light impinging on the sphere surface is diffusely reflected, and

the detector can be placed anywhere in the sphere in order to gather the average flux [36–39]. By inserting an absorbing medium in the cavity, a reduction of the radiance in the sphere occurs. The reduction is related only to the absorption of the sample and to its volume, and is independent of scattering, which does not change the average radiance in the cavity. This technique has been recently proposed for effective gas analyses [40, 41].

Efficient diffuse-light measurements need bright sources. A conventional deuterium/halogen lamp is enough, provided that it is butt-coupled to the integrating sphere. However, when optical fibers are needed for a better geometrical versatility of the measuring system, conventional lamps provide poor and insufficient light intensity.

In order to overcome insufficient lighting, we used a compact, high-brightness *supercontinuum* fiber optic source, the revolutionary advent of which has recently changed the perspectives of optical spectroscopy [42, 43]. This innovative source is made of a holey optical fiber, typically a photonic crystal fiber, which is pumped by a high-power nano- or femtosecond laser. The bright light generated by the holey fiber over a wide spectral range was guided to the input port of the integrating sphere. Another port of the sphere accommodated an optical fiber coupled to a spectrometer, so as to achieve an efficient set-up for diffuse-light absorption spectroscopy, as shown in Fig. 1. The detected light-power, P , is described by Equation 1, as:

$$P = \frac{R P_0 A_d}{S} \frac{1}{1 - \frac{R}{S} (S - A_s - \alpha V)} \quad (1)$$

where P_0 is the source power; α is the sample absorption coefficient; V is the sample volume; A_d is the detector fiber area; A_s is the source fiber area; R is the cavity power reflectivity; S is the cavity surface area.

Commercially available components were used for the practical implementation of the experimental set-up [44].

Fig. 1 Set-up for diffuse-light absorption spectroscopy by means of optical fiber technology

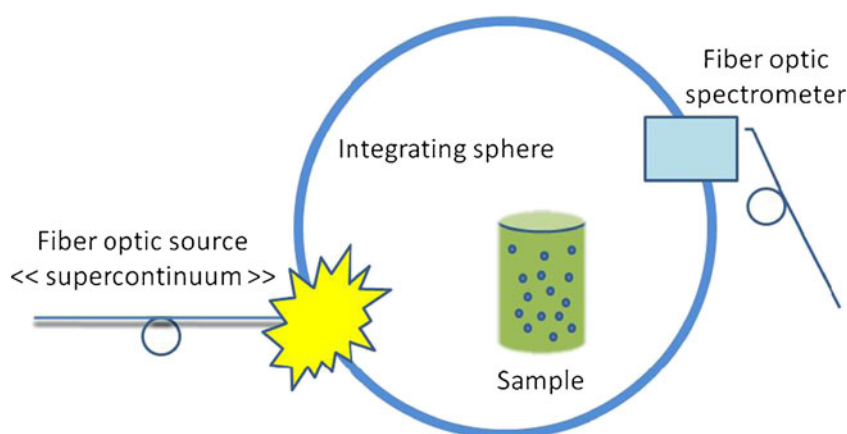


Table 1 Codes of experimented authentic EVOOs and adulterants

Code	Type of oil
O1	EVOO from Tuscany
O2	EVOO from Tuscany
O3	EVOO from Tuscany
O4	EVOO from Tuscany
F1	OPO
F2	ROO
F4	DOO
F5	ROPO

The Fianium-SC400 fiber optic *supercontinuum* source was used for illumination: it emits 4 W throughout the entire 415–1,800 nm spectral range. The Instrument System-Spectro 320 fiber optic spectrometer was used as detector, and scanned the wide 400–1,700 nm spectral range with a resolution of 1.37 nm. The Labsphere LMS100 cavity was used as a diffusing sphere, the ports of which were equipped by means of fiber optic connectors for coupling to both the source and the detector. The olive oil sample under test was contained in a glass vial having a volume of 32 cm³. This set-up was previously used for lubricant oil analysis—it allowed for a successful spectral fingerprinting

of the lubricant oil and for predicting functional parameters and wear indicators [45].

The collection of authentic extra virgin olive oils and adulterants

Authentic EVOOs were four different types of oils collected in Tuscany, which were produced according to local traditions around the area of Grosseto. The lower-grade olive oils, OPO, ROO, ROPO, and DOO, were provided by the Università di Udine. Table 1 summarizes the codes used for identifying the various oil types.

Four series of EVOO-adulterant mixtures were prepared. Each of them was made of five samples in which the adulterant fraction was 0.05, 0.25, 0.50, 0.75, and 0.95 of total weight, respectively. They were used for calibration procedures. For each series, three replica mixtures of EVOOs with 0.25, 0.50, 0.75 in weight of adulterants were also prepared. These provided a validation set for the regression model. The entire collection of measured oils consisted of 136 samples, 88 for calibration and 48 for validation, respectively.

Fig. 2 Diffuse-light absorption spectra: entire collection of authentic EVOOs (a), adulterants (b), O1F1 mixtures giving similar spectra (c), and O1F4 mixtures giving very different spectral signatures (d)

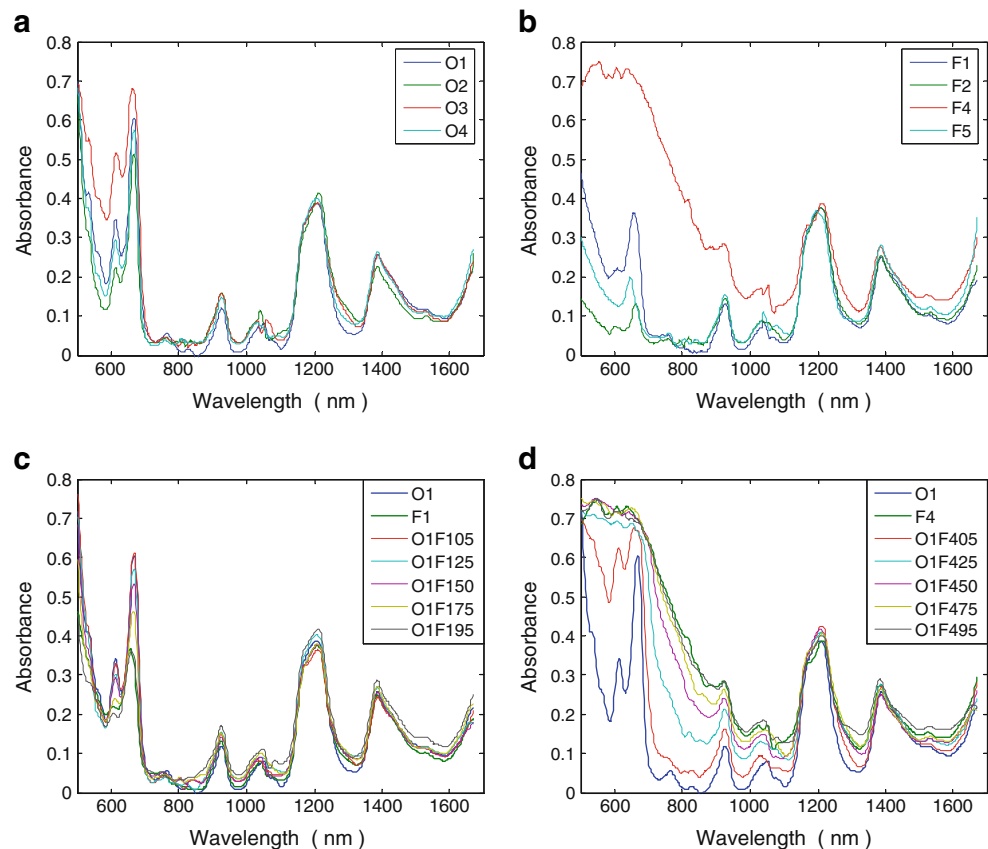


Table 2 Summary of parameters for predicting the fraction of adulterant by means of optical spectroscopy

EVOO-adulterant mix	# PF	RMSEC	RMSEP	R^2
O1F1	1	0.09	0.05	0.947
O1F2	1	0.06	0.07	0.975
O1F4	2	0.07	0.05	0.971
O1F5	1	0.07	0.13	0.964
O2F1	2	0.03	0.06	0.996
O2F2	1	0.01	0.06	0.933
O2F4	2	0.07	0.06	0.969
O2F5	2	0.02	0.08	0.997
O3F1	2	0.02	0.05	0.996
O3F2	2	0.02	0.02	0.997
O3F4	2	0.05	0.04	0.985
O3F5	1	0.10	0.10	0.932
O4F1	1	0.10	0.03	0.926
O4F2	1	0.07	0.07	0.966
O4F4	2	0.07	0.06	0.968
O4F5	2	0.04	0.08	0.990

For every sample, an empty vial was used to measure P_0 , which was replaced by the vial containing the sample under test to measure P . The diffuse-light absorbance, A , hereinafter referred to absorbance only, was calculated as:

$$A = \frac{P_0}{P} - 1 \quad (2)$$

for obtaining a quantity which is linearly related to α , also having $A=0$ when there is no attenuation, as in conventional absorption spectroscopy.

Figure 2-top shows the measured diffuse-light absorption spectra of all authentic EVOOs and adulterants. Their mixtures show intermediate spectra: as an example, Fig. 2-bottom shows the O1 EVOO adulterated by means of two different adulterants, OPO and DOO, respectively, providing very similar (O1F1 mix) or highly different (O1F4 mix) spectral signatures. A multivariate processing of the

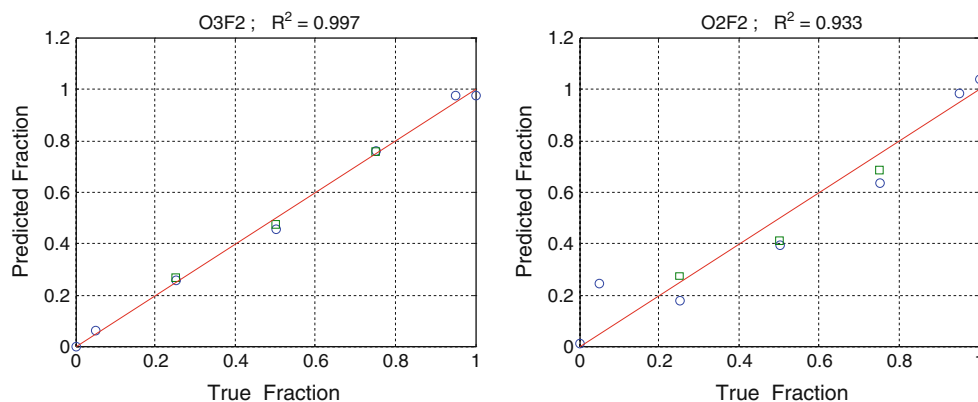
spectroscopic data allowed for predicting the fraction and the type of adulterant. All data processing was carried out in MATLAB® code, by means of customized programs.

Predicting the fraction of adulterant

As a first processing, the spectra were smoothed by means of Savitsky–Golay algorithm, employing a second degree polynomial and a smoothing window of 15 points (30 nm). Then, the prediction of the adulterant fraction in the mixtures was achieved by using a multivariate analysis method called *partial least squares* regression (PLS) [46]. This method is used when the predictor matrix has many collinear variables and the usual multiple linear regression cannot be applied. PLS looks for a limited number of PLS “factors” (PF) which are linear combinations of the original predictors. These new variables are mutually orthogonal (thus uncorrelated) and have the maximum possible covariance with the target variable, among all possible combinations of the original predictors. The idea is that each PF should be linked to a different source of data variance, with the first PF being the most linked to the target variable.

The estimation of the optimal number of factors needed to fit the data is a critical issue of PLS. In our experiment, theoretical considerations suggested that only one factor should be needed, because the only “physical” cause for the variability of absorbance was the adulterant fraction. However, due to the presence of saturated absorption peaks, the relation between absorbance and adulterant fraction was not strictly linear (and PLS is a linear method), and one additional PF was sometimes needed to compensate for non linearity. This was particularly evident for F4, which showed the strongest absorption among all the analyzed oils. The optimal number of factors was assessed by testing each PLS model on the validation set and by choosing that minimized the root mean square error of prediction (RMSEP). Two other parameters were evaluated

Fig. 3 Linear regression between true and predicted fraction of adulterant: the best (O3F2) and the worst (O2F2) cases (circles calibration points, squares validation points)



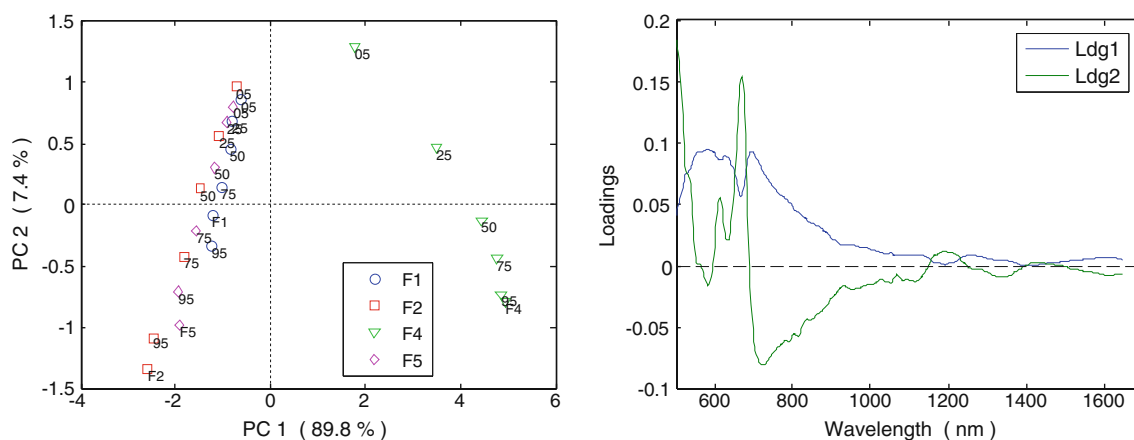


Fig. 4 Results of PCA processing obtained for O1 calibration EVOO—*left* PCA score plot; *right* relative loadings

in order to assess the goodness of the fit: the root mean square error of calibration (RMSEC) and the determination coefficient (R^2). RMSEC is, like RMSEP, an estimation of the “expected” prediction error, but is evaluated on the calibration set. R^2 is, instead, the squared correlation coefficient between predicted and reference values, for the calibration set; thus the fit is as better as this value is closer to 1.

Table 2 summarizes the values of these parameters for each EVOO-adulterant mixture, together with the chosen number of PF (# PF). Note that all mixtures involving F4 needed two PFs for achieving the best fit. Indeed, all values of R^2 are very good. The best prediction is obtained for O3 EVOO adulterated by means of ROO (F2), showing $R^2=0.997$ and RMSEP=0.02. The worst prediction, which is still very good, is obtained for O3 EVOO adulterated by means of ROPO (F5), showing $R^2=0.932$ and RMSEP=0.1. Figure 3 shows the linear regression graphics of these two cases.

Discriminating the type of adulterant

The previous section showed how it is possible to predict the fraction of adulterant when the adulterant type is known a priori. However, in practice, the type of adulterant is usually unknown. Therefore, we investigated how to discriminate among the different types of adulterants by means of multivariate calibration and classification methods [47].

The *principal component analysis* (PCA) was firstly used for data exploration. For each EVOO, the spectra of pure adulterants and of calibration mixtures were considered, thus taking into account 24 samples. Figure 4 shows the results of PCA processing obtained for O1 EVOO; similar results were obtained for the other EVOOs. Figure 4-left shows the PCA score plot, and Fig. 4-right the relative loadings. The score plot highlights that DOO (the F4 adulterant) can be easily distinguished along the PC1 axis. In fact, as shown by the loadings, PC1 is linked to the

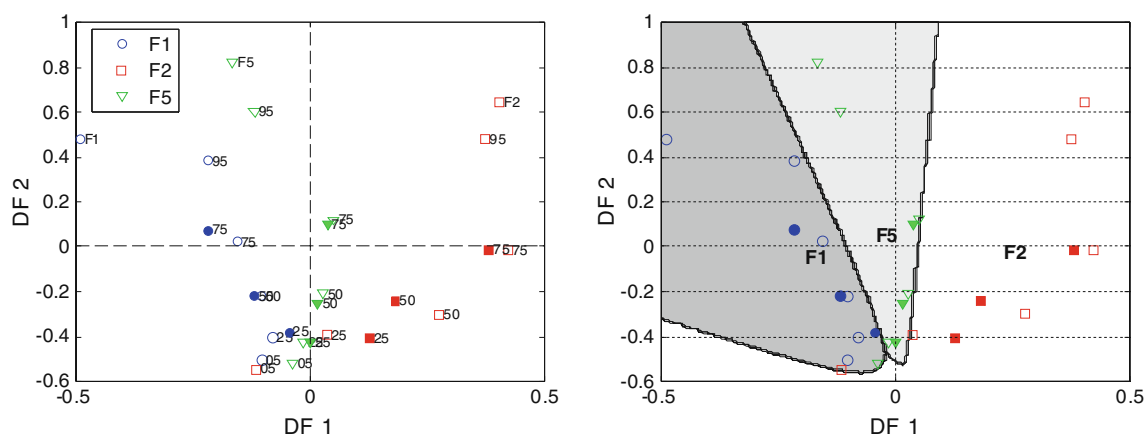


Fig. 5 Results of PCA+LDA processing for discriminating OPO, ROO, and ROPO (F1, F2, and F5) in O1 EVOO (empty and filled dots represent the calibration and validation samples, respectively)—

left discriminating map with labels indicating the adulterant percentage in the mixture; *right* discriminating map with boundaries

Table 3 Errors of OPO, ROO, and ROPO classification for each authentic EVOO, for both the calibration and the validation set

EVOO	Calibration set errors	Validation set errors
O1	2	0
O2	2	1
O3	10	6
O4	3	2

average absorbance in the 500–900 nm range, where DOO absorbance is higher and broader than any other adulterant.

However, for a better discrimination of the other three adulterants, a more dedicated method such as the *linear discriminant analysis* (LDA) was needed. Since overfitting is likely with LDA direct processing of large variable sets, like spectra, a two-step PCA+LDA model was considered. For each EVOO, calibration and validation sets were created. The calibration set was made by the spectra of pure OPO, ROO, and ROPO adulterants, and of the relative calibration mixtures (total 18 samples), while the validation set was made by the validation mixtures of the same adulterants (total 9 samples). PCA was applied to the calibration set, showing that two PCs only were sufficient to obtain explained variances of 96% or higher in any case. LDA was then performed on the PCA score matrix, obtaining two discrimination functions. Finally, the decision boundaries separating the three classes of adulterants were calculated. Figure 5 shows the results of PCA+LDA processing for discriminating OPO, ROO, and ROPO (F1, F2, and F5) in O1 EVOO; similar figures were obtained for the other EVOOs. Empty and filled dots represent the calibration and validation samples, respectively. Figure 5-left shows the discriminating map: labels indicating the adulterant percentage in the mixture are added, while adulterants are simply identified by their code. Figure 5-

Table 5 Summary of parameters for predicting the fraction of adulterant by means of gas chromatography

EVOO-adulterant mix	# PF	RMSEC	RMSEP	R ²
O1F1	1	0.02	0.03	0.997
O1F2	1	0.04	0.05	0.989
O1F4	1	0.03	0.04	0.994
O1F5	1	0.03	0.04	0.993
O2F1	1	0.02	0.03	0.996
O2F2	1	0.03	0.03	0.993
O2F4	1	0.03	0.03	0.996
O2F5	1	0.03	0.03	0.995
O3F1	1	0.02	0.03	0.996
O3F2	1	0.03	0.04	0.993
O3F4	1	0.03	0.04	0.995
O3F5	1	0.03	0.04	0.995
O4F1	1	0.02	0.03	0.996
O4F2	1	0.03	0.04	0.994
O4F4	1	0.02	0.04	0.995
O4F5	1	0.03	0.03	0.994

right shows the discriminating map also including the discriminating boundaries.

As expected, the best discrimination among the adulterants is achieved with high adulterant concentrations, and the dots converge towards a point where the pure EVOO should be. Note that the spectrum of authentic EVOO was not considered in the LDA processing, for not introducing a fourth class populated by a single element, which contrasts with LDA principles.

Table 3 summarizes the errors of classification for each authentic EVOO, for both the calibration and the validation set. The errors for the calibration set are higher because this set includes the samples with 0.05 adulterant fraction, which are the most difficult to separate.

Table 4 Summary of fatty acid composition for authentic EVOOs and adulterant oils

Fatty acid content	O1 (%)	O2 (%)	O3 (%)	O4 (%)	F1 (%)	F2 (%)	F4 (%)	F5 (%)
Palmitic	13.70	13.00	12.90	13.80	11.63	13.92	9.90	11.94
Palmitoleic	1.20	1.10	1.00	1.00	0.92	1.64	0.38	0.92
Eptadecanoic	0.04	0.03	0.03	0.03	0.06	0.08	0.03	0.06
Eptadecenoic	0.06	0.05	0.05	0.05	0.11	0.16	0.05	0.09
Stearic	2.30	2.40	2.20	2.40	2.62	2.24	2.50	2.31
Oleic	73.10	74.00	72.60	73.40	72.58	71.05	75.60	72.42
Linoleic	8.40	8.30	7.20	8.00	10.63	9.60	9.86	10.92
Arachidic	0.30	0.30	0.30	0.30	0.43	0.38	0.42	0.39
Linolenic	0.60	0.50	0.60	0.60	0.50	0.54	0.65	0.46
Eicosenoic	0.20	0.20	0.30	0.20	0.28	0.23	0.36	0.28
Behenic	0.07	0.10	0.10	0.10	0.17	0.11	0.18	0.16
Lignoceric	0.03	0.02	0.02	0.02	0.07	0.05	0.07	0.05

The discrimination of OPO, ROO, and ROPO adulterants in O1, O2, and O4 EVOOs is very good, while it worsens for O3. Since O3, unlike the other EVOOs, has an absorbance sensibly higher than all adulterants (except DOO, which is not considered here), the main effect of O3 spiking, whichever adulterant is used, is a general lowering of absorbance, which masks more subtle changes in the spectrum shape.

Comparison of optical spectroscopy analysis with capillary gas chromatography

In order to evaluate the effectiveness of optical spectroscopy with respect to other standard methods, a capillary gas chromatographic analysis of fatty acid composition was carried out. In fact, the determination of fatty acids proved to be a valid technique for the classification of vegetable oils and for the detection of adulteration [48, 49].

The fatty acid composition of the entire collection of olive oils was determined by using the HRGC MEGA 2 series Fisons Instruments. The fatty acid composition was determined as the corresponding methyl esters, which were prepared by means of an alkaline treatment carried out by mixing 0.05 g of oil dissolved in 2 ml of *n*-hexane with 1 ml of 2 N potassium hydroxide in methanol [50, 51]. A fused silica capillary column (50 m in length, 0.25 mm i. d.), coated by CPSil-88 (0.25 μ m film thickness, Varian Palo Alto, CA) was utilized. Table 4 summarizes the fatty acid composition of authentic EVOOs and adulterants. An ANOVA test [52] was carried out to detect significant differences in fatty acid content between authentic EVOOs and adulterants. The following four fatty acids: linoleic, arachidic, behenic, and lignoceric showed substantial differences at a significance level of 5%.

In order to predict the fraction of adulterant, a PLS regression algorithm was used, which employed the fatty acid composition as the predictor pattern. For every EVOO-adulterant mixture, the best fit was achieved by using a single PF. The values of fit statistics (RMSEC, RMSEP, R^2) are summarized in Table 5. As expected, the gas chromatographic analysis showed an accurate prediction of the adulterant fraction. However, the results obtained by means of optical spectroscopy, without any sample treatment, are comparable with those obtained using the standard method.

Perspectives

Diffuse-light absorption spectroscopy performed in the 400–1,700 nm spectral range, combined with a multivariate processing of spectroscopic data, have demonstrated the capability of predicting the adulteration and concentration

of diverse lower-grade olive oils which are frequently used as adulterants of authentic EVOOs produced in Tuscany, a centrally located Italian region. Being scattering-independent, this technique can be used for EVOO analysis during the entire shelflife of the product.

The obtained results are encouraging, especially because of the chemical similarities of authentic EVOOs and the lower-grade olive oils considered as adulterants. To the best of our knowledge, we have demonstrated for the first time that optical spectroscopy can be successfully used to quantify the fraction of DOO in authentic EVOO. It is an innovative result, especially in view of the growing use of DOO as adulterant. We are currently considering other types of adulterants, as well as authentic EVOOs from other regions for achieving a wider data base.

Verifying the authenticity of EVOOs is just one of the many other potential applications that diffuse-light absorption spectroscopy has, especially in combination with a suitable processing of the spectroscopic data. Other types of expensive foodstuffs can be authenticated, such as bio-juices, honeys, alcoholic beverages, as well as many other liquids, the most promising of which can be dietary supplements based on herbs and natural cosmetics.

Acknowledgments The authors are grateful to the following initiatives for partial financial support: EC Network of Excellence on Micro-Optics (NEMO), EC Network of Excellence for Biophotonics (P4L), CNR Short-Term Mobility Program 2009, and A.R.S.I.A. Mr. Franco Cosi is acknowledged for technical support.

References

1. Willett WC (1998) Nutritional epidemiology, 2nd ed., vol. 30 of Monographs in Epidemiology and Biostatistics. Oxford University Press, New York
2. Paiva-Martins F, Fernandes J, Rocha S, Nascimento H, Vitorino R, Amado F, Borges F, Belo L, Santos-Silva A (2009) Effects of olive oil polyphenols on erythrocyte oxidative damage. *Mol Nutr Food Res* 53(5):609–616
3. Gimeno E, Fitó M, Lamuela-Raventós RM, Castellote AI, Covas M, Farré M, de La Torre-Boronat MC, López-Sabater MC (2002) Effect of ingestion of virgin olive oil on human low-density lipoprotein composition. *Eur J Clin Nutr* 56:114–120
4. Covas MI (2007) Olive oil and the cardiovascular system. *Pharmacol Res* 55:175–186
5. Commission Regulation EEC n. 2568/91 and subsequent amendments, online: <http://eur-lex.europa.eu/LexUriServ/site/en/consleg/1991/R/01991R2568-20031101-en.pdf>.
6. Fasciotti M, Pereira Netto AD (2010) Optimization and application of methods of triacylglycerol evaluation for characterization of olive oil adulteration by soybean oil with HPLC-APCI-MS-MS. *Talanta* 81:1116–1125
7. Agiomyrgianaki A, Petrakis PV, Dais P (2010) Detection of refined oil adulteration with refined hazelnut oil by employing NMR spectroscopy and multivariate statistical analysis. *Talanta* 80:2165–2171
8. Priego Capote F, Ruiz Jiménez J, Luque de Castro MD (2007) Sequential (step-by-step) detection, identification and quantitation

- of extra virgin olive oil adulteration by chemometric treatment of chromatographic profiles. *Anal Bioanal Chem* 388:1859–1865
9. Jafari M, Kadivar M, Keramat J (2009) Detection of adulteration of Iranian olive oil using instrumental (GC, NMR, DSC) methods. *Journal of the American Oil Chemist Society* 86:103–110
 10. Angiuli M, Bussolino GC, Ferrari C, Matteoli E, Righetti MC, Salvetti G, Tombari E (2009) Calorimetry for fast authentication of edible oils. *Int J Thermophys* 30:1014–1024
 11. Chiavaro E, Vittadini E, Rodriguez-Estrada MT, Cerretani L, Bendini A (2008) Differential scanning calorimeter application to the detection of refined hazelnut oil in extra virgin olive oil. *Food Chem* 110:248–256
 12. Ferrari C, Angiuli M, Tombari E, Righetti MC, Matteoli E, Salvetti G (2007) Promoting calorimetry for olive oil authentication. *Thermochim Acta* 459:58–63
 13. Lizhi H, Toyoda K, Ihara I (2010) Discrimination of olive oil adulterated with vegetable oil using dielectric spectroscopy. *J Food Eng* 96:167–171
 14. Marina AM, Che Man YB, Amin I (2010) Use of the SAW sensor electronic nose for detecting the adulteration of virgin coconut oil with RDB palm kernel olein. *Journal of the American Oil Chemistry Society* 87:263–270
 15. Hai Z, Wang J (2006) Electronic nose and data analysis for detection of maize oil adulteration in sesame oil. *Sensors and Actuators B* 119:449–455
 16. Lerma-Garcia MJ, Ramis-Ramos G, Herrero-Martinez JM, Simò-Alfonso EF (2010) Authentication of extra virgin olive oils by Fourier-transform infrared spectroscopy. *Food Chem* 118:78–83
 17. Vlachos N, Skopelitis Y, Psaroudaki M, Konstantinidou V, Chatzilazarou A, Tegou E (2006) Applications of Fourier transform-infrared spectroscopy to edible oils. *Anal Chim Acta* 573–574:459–465
 18. Gurdeniz G, Ozen B (2009) Detection of adulteration of extra-virgin olive oil by chemometric analysis of mid-infrared spectral data. *Food Chem* 116:519–525
 19. Ozdemir D, Ozturk B (2007) Near infrared spectroscopic determination of olive oil adulteration with sunflower and corn oil. *Journal of Food and Drug Analysis* 15(1):40–47
 20. Poulli KI, Mousdis GA, Georgiou CA (2007) Rapid synchronous fluorescence method for virgin olive oil adulteration assessment. *Food Chem* 105:369–375
 21. Guimet F, Ferré J, Boqué R (2005) Rapid detection of olive-pomace oil adulteration in extra virgin olive oils from the protected denomination of origin *Siurana* using excitation-emission fluorescence spectroscopy and three-way methods of analysis. *Anal Chim Acta* 544:143–152
 22. Christy AA, Kasemsumran S, Du Y, Ozaki Y (2004) The detection and quantification of adulteration in olive oil by near-infrared spectroscopy and chemometrics. *Anal Sci* 20:935–940
 23. Sayago A, Morales MT, Aparicio R (2004) Detection of hazelnut oil in virgin olive oil by a spectrofluorimetric method. *Eur Food Res Technol* 216:480–483
 24. Downey G, McIntyre P, Davies AN (2002) Detecting and quantifying sunflower oil adulteration in extra virgin olive oils from the Eastern Mediterranean by visible and near-infrared spectroscopy. *J Agric Food Chem* 50:5520–5525
 25. Maggio RM, Cerretani L, Chiavaro E, Kaufman TS, Bendini A (2010) A novel chemometric strategy for the estimation of extra virgin olive oil adulteration with edible oils. *Food Control* 21:890–895
 26. Bucci R, Magri AD, Magri AL, Marini D, Marini F (2002) Chemical authentication of extra virgin olive oil varieties by supervised chemometric procedures. *J Agric Food Chem* 50:413–418
 27. Galtier O, Dupuy N, Le Dréau Y, Olliver D, Pinatel C, Kister J, Artaud J (2007) Geographic origins and compositions of virgin olive oils determined by chemometric analysis of NIR spectra. *Anal Chim Acta* 595:136–144
 28. Guimet F, Ferré J, Boqué R, Rius FX (2004) Application of unfold principal component analysis and parallel factor analysis to the exploratory analysis of olive oils by means of excitation–emission matrix fluorescence spectroscopy. *Anal Chim Acta* 515:75–85
 29. Torrecilla JS, Rojo E, Dominguez JC, Rodriguez F (2010) A novel method to quantify the adulteration of extra virgin olive oil with low-grade olive oils by UV–VIS. *J Agric Food Chem* 58:1679–1684
 30. Mellon MG (1950) *Analytical absorption spectroscopy*. Wiley, New York
 31. Bauman RP (1962) *Absorption spectroscopy*. Wiley, New York
 32. Mark H, Workman J Jr (2003) *Statistics in spectroscopy*, 2nd edn. Academic, San Diego
 33. Fecht I, Johnson M (1999) Non-contact scattering independent water absorption measurement using a falling stream and integrating sphere. *Meas Sci Technol* 10:612–618
 34. Merzlyak MN, Razi Naqvi K (2000) On recording the true absorption spectrum and the scattering spectrum of a turbid sample: application to cell suspensions of the cyanobacterium *Anabaena variabilis*. *J Photochem Photobiol, B* 58:123–129
 35. Jávorfí T, Eröstyák J, Gál J, Buzády A, Menczel L, Garab G, Razi Naqvi K (2006) Quantitative spectrophotometry using integrating cavities. *J Photochem Photobiol, B* 82:127–131
 36. Elterman P (1970) Integrating cavity spectroscopy. *Appl Opt* 9:2140–2142
 37. Fry ES, Kattawar GW, Pope RM (1992) Integrating cavity absorption meter. *Appl Opt* 31:2055–2065
 38. Nelson NB, Prézelin BB (1993) Calibration of an integrating sphere for determining the absorption coefficient of scattering suspensions. *Appl Opt* 32:6710–6717
 39. Kirk JTO (1995) Modeling the performance of an integrating-cavity absorption meter: theory and calculations for a spherical cavity. *Appl Opt* 34:4397–4408
 40. Hawe E, Fitzpatrick C, Chambers P, Dooly G, Lewis E (2008) Hazardous gas detection using an integrating sphere as a multipass gas absorption cell. *Sensors & Actuators A* 141:414–421
 41. Hodgkinson J, Masiyano D, Tatam RP (2009) Using integrating spheres as absorption cells: path-length distribution and application of Beer's law. *Appl Opt* 48:5748–5758
 42. Alfano AR (ed) (2006) *The supercontinuum laser source*, 2nd edn. Springer, Berlin
 43. Kaminski CF, Watt RS, Elder AD, Frank JH, Hult J (2008) *Supercontinuum radiation for applications in chemical sensing and microscopy*. *Appl Phys B* 92:367–378
 44. Source: <http://www.fianium.com/> - Detector: <http://www.instrumentsystems.com/>—integrating sphere: <http://www.labsphere.com/>
 45. Mignani AG, Ottevaere H, Ciaccheri L, Thienpont H, Cacciari I, Parriaux O, Johnson M (2009) Innovative spectroscopy of liquids: a fiber optic supercontinuum source and an integrating cavity for scattering-free absorption measurements, *Proc. SPIE vol. 7503 20th International Conference on Optical Fibre Sensors*, pp. 750377-1/4.
 46. Wold S, Sjostrom M, Eriksson L (2001) PLS-regression: a basic tool for chemometrics. *Chemom Intell Lab Syst* 58:109–130
 47. Naes T, Isaksson T, Fearn T, Davies T (2002) *Multivariate calibration and classification*. NIR Publications, Chichester
 48. Brodnjak-Voncina D, Cencic-Kodba Z, Movic M (2005) Multivariate data analysis in classification of vegetable oils characterized by the content of fatty acids. *Chemom Intell Lab Syst* 75:31–43
 49. Christopoulou E, Lazaraki M, Komaitis M, Kaselimis K (2004) Effectiveness of determinations of fatty acids and triglycerides for

- the detection of adulteration of olive oils with vegetable oils. *Food Chem* 84:463–474
50. Bendini A, Cerretani L, Vecchi S, Carrasco-Pancorbo A, Lercker G (2006) Protective effects of extra virgin olive oil phenolics on oxidative stability in the presence or absence of copper ions. *J Agric Food Chem* 54:4880–4887
 51. Christie WW (1998) *Gas Chromatography and lipids: a practical guide*, The Oily Press, Bridgewater, Somerset, UK, on line: <http://www.pjbarnes.co.uk/free/GasChromatographyAndLipids.pdf>.
 52. Vandeginste BGM, Massart DL, Buydens LCM, De Jong S, Lewi DJ, Smeyers-Verbeke J (1998) *Handbook of chemometrics and qualimetrics*. Elsevier, Amsterdam